

Canine Left Ventricular Purkinje Fiber Network Construction Using Manifold Learning

J Li¹, KQ Wang¹, WM Zuo¹, YF Yuan¹, HG Zhang²

¹Harbin Institute of Technology, Harbin, China

²University of Manchester, Manchester, UK

Abstract

Purkinje fiber network (PFN), one of the most important components of the ventricular conduction system, is crucial in modeling ventricular tachycardia and fibrillation. Construction of anatomical detail Purkinje fiber network, however, is a very challenging task. In this paper, we present a novel method for restoring the 3D PFN in the left ventricle (LV) by manifold learning. Motivated by the fact that canine Purkinje fiber is generally on the endocardial surface of the heart, we have collected a set of real 2D canine LV images, from which the PFN image is detected and segmented. We then use manifold learning to map 3D canine left ventricular model to 2D PFN and the inverse mapping to finish the final construction. Our experimental results show that the 3D PFN construction method is flexible and feasible.

1. Introduction

Purkinje fiber network in the canine left ventricle, which includes the left bundle branch and the Purkinje fiber, lies in the endocardial layer, and can be hardly seen whether from outer space or from the inner space of the ventricle. Traditional medical imaging methods, such as magnetic resonance imaging (MRI) or computed tomography (CT), can be used to obtain the 3D structure information of the LV, but fail to reveal the PFN information.

Because of the great significance of the PFN in modeling ventricular tachycardia and fibrillation, so far, there have been several PFN reconstruction methods.

Siregar et al. developed a simplified model which was composed of few branches connecting the sites directly to the branches and bundle (Figure. 1A) [1]. Simelius et al. incorporated a detailed anatomically based PFN system in human ventricles model, where the organization of the conduction system was from textbooks on human anatomy and PFN is supposed to be in almost the same width (Figure. 1B) [2]. Recently, Vigmond and Clements developed an anatomically based Purkinje system for the

San Diego rabbit ventricles model by flattening the endocardial surfaces onto a plane using a multidimensional scaling method, and PFN was also drawn manually (Figure. 1C) [3].

In this paper, we propose a novel method to construct PFN by means of real canine PFN data. To ensure that the local structure of PFN is preserved, we use the locally linear embedding (LLE) algorithm resulting in that the original 3D data on the endocardial surface is mapped to a 2D plane. We rescale, rotate and translate the measurement of the plane surface to make it consistent to the PFN image.

The discrete PFN image is embedded on the 3D curved surface using the main bundle branches and boundaries as markers. When we successfully obtain a PFN-embedded plane surface image, we will use the inverse LLE mapping to represent the 3D PFN which is within the 3D LV muscle. Finally, anatomical detail 3D Purkinje fiber network is obtained with a satisfactory visible quality.

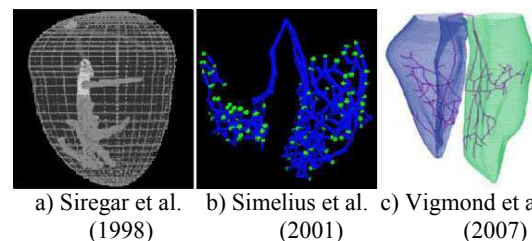


Figure 1. Images of PFN construction from different institutions

2. LLE

Manifold learning, which attempts to recover a lower dimensional manifold from data points in a high dimensional space, have generated techniques such as Isomap [4], locally linear embedding (LLE) [5,6], and Hessian LLE [7]. Among them, LLE keeps locally linear relationship very well between points in high dimensional space, and recovers global nonlinear structure from locally linear fits, that is the reason we choose it in our method.

Suppose the data set consists of a set of D -dimensional vectors $\{X_1, \dots, X_M\}$ sampled from some underlying manifold. M is the number of elements in the set. Provided there are sufficient data, we expect each data point and its neighbors to lie on or close to a locally linear patch of the manifold. We characterize the local geometry of these patches by linear coefficients which are used to reconstruct a data point from its neighbors.

Reconstruction errors are measured by the cost function

$$\varepsilon(W) = \sum_{i=1}^M \left| X_i - \sum_j W_{ij} X_j \right|^2 \quad (1)$$

The weights W_{ij} summarize the contribution of the j th data point to the i th reconstruction. To compute the weights W_{ij} , we minimize the cost function with the following two constraints:

First, each data point X_i is reconstructed only from its neighbors by enforcing $W_{ij}=0$ if X_j does not belong to the set of neighbors of X_i . Second, sum of each row of the weight matrix is one, $\sum_j W_{ij} = 1$. The optimal weights W_{ij} subjected to these constraints are obtained by solving a least-squares problem.

LLE constructs a neighborhood-preserving mapping. In the final step of the algorithm, each high-dimensional observation X_i is mapped to a low-dimensional vector Y_i by preserving global internal manifold structure and choosing D -dimensional coordinates Y_i to minimize the embedding cost function

$$\Phi(Y) = \sum_{i=1}^M \left| Y_i - \sum_j W_{ij} Y_j \right|^2 \quad (2)$$

This cost function, like the previous one, is based on locally linear reconstruction errors, but here we fix the weights W_{ij} while optimizing the coordinates Y_i . The embedding cost in Eq. (2) defines a quadratic form in the vectors Y_i . With the constraints that make the problem well-posed, it can be minimized by solving a sparse $M \times M$ eigenvalue problem, where the eigenvectors with the D smallest nonzero eigenvalues provide an ordered set of orthogonal coordinates centered on the origin.

3. PFN Construction

The geometry of the left endocardial surfaces was based on the Canine heart model of Cornell University (<http://thevirtualheart.org/>). Our PFN construction method includes the following main steps:

- 1) PFN extraction: The points of PFN are extracted from the collected canine LV image. The extracted points are collected to construct a points set C .
- 2) Mapping from 3D surface, which is composed of the points-set P , to 2D LV plane, which is composed of the points-set F : This step includes locally linear embedding and tracking of the boundary points.
- 3) Match with P and C , and obtaining new 2D plane image Z after embedding C to P .

- 4) Inverse Mapping: This step map Z to 3D space.

The result of Step 2 provided us with a one-to-one mapping of the 3D points to the points in a plane; the inverse of this mapping was used in Step 4. In the following, we discuss each of these steps in detail.

In the following, we discuss each of these steps in detail.

3.1. PFN extraction from the canine LV image

In the PFN images, the PFN lying in the endocardial layer of a canine LV, as is shown in Figure. 2a. The anatomical detail linear shape of PFN is extracted by means of the semi-automated method, as the following two steps:

- 1) Extracting the profile of PFN by the threshold value of the gray scale, and region-dependant segmentation.
- 2) Extracting each segment using different threshold values, till the branches are extracted. Close to the termination of each branch, the gray scale of the branch point is similar to the one of background. Thus it is necessary to modify the gray information of points in termination branches.
- 3) Combining all the segmentations to the whole image, points of which are marked as the points-set C .

The image of the points-set C is shown in Figure. 2b.

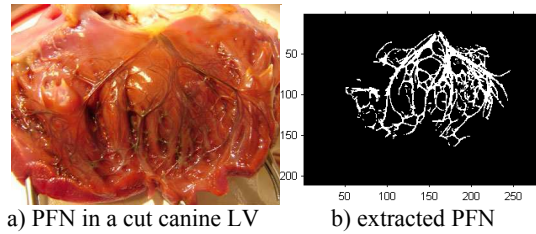


Figure 2. 2D information of PFN

3.2. Mapping from 3D surface to 2D LV plane

3.2.1. Mapping from 3D points-set F to 2D points-set P .

- 1) Compute the k neighbors of each data point X_i in F .
- 2) Compute the weights W_{ij} that best reconstruct each data point X_i from its neighbors.
- 3) Compute the vectors Y_i , which make up of P , using the LLE algorithm.

The number of neighbours, k , is crucial in the algorithm, which determine the distribution of the points-set F in 2D space. We experimentally determine the optimal k value from a predefined numerical range.

3.2.2. Obtaining boundary points-set Pb of P, Fb of F.

It is easy to obtain the boundary of the 2D points-set P ,

$$Pb = \{p_i | p_i \in P, p_i \text{ is a boundary point of the image composed of } P\} .$$

Since the points of F have one-to-one correspondence to the points of P in Section 3.2.1, Fb can be obtained from the mapping obtained:

1) The polar coordinate is created. In order to find the boundary faster, geometric centre of P is taken as the origin of the polar coordinate:

$$(x_o, y_o) | x_o = \sum_{i=1}^M x_i / M, y_o = \sum_{i=1}^M y_i / M, \quad (3)$$

where M is the number of the point in P .

2) The other points in the set P , transform their rectangular coordinates into the polar coordinates. The angle α_i and radius r_i of point $[x_i, y_i]^T$ is described as:

$$\alpha_i = \arctan((y_i - y_o) / (x_i - x_o)) \quad (4)$$

$$r_i = \sqrt{(y_i - y_o)^2 + (x_i - x_o)^2} \quad (5)$$

3) We divide the points of the set P into n subsets according to their angle values. In the i th subset is defined as

$$A_i = \left\{ P_j \in P \mid -\pi + \frac{2(i-1)}{n} \pi \leq \alpha_j \leq -\pi + \frac{2i}{n} \pi \right\} \quad (6)$$

If the number of points is m_i , then the boundary points Pb_i are probably among ones with the largest radius in the subset:

$$Pb_i = \max_{1 \leq j \leq m_i} \{r_j | P_j \in A_i\} . \quad (7)$$

4) Points distribution of set P is not evenly distributed, which consequently makes some subsets have few points, that means, not all Pb_i in the subsets from the above are the real boundary points. Therefore, we introduce a variable t for the refinement of Pb_i :

When $m_i < t$, merge A_i with A_{i+1} till $m_i \geq t$

$$A_i = A_i \cup A_{i+1} \quad (8)$$

$$m_i = m_i + m_{i+1} \quad (9)$$

5) When the points-set P is obtained from F by LLE algorithm, that is $L: F \rightarrow P$, furthermore, $F \leftrightarrow P$, and $L(F_i) = P_i, i=1, \dots, M$, so the boundary points-set Fb can be obtained from Pb .

3.3. Matching P and C, and obtaining new 2D image H after embedding C to P.

3.3.1. Setting position of the 2D points-set C.

For mathematical manipulation conveniency, point of C , $[x, y]^T$, is expressed as $[x, y, 1]^T$. After the scale transform K , rotation transformation R , translation transformation T , C turns to be C^* :

$$C^* = T \circ R \circ K(C) \quad (10)$$

$$T = \begin{bmatrix} 1 & 0 & x_d \\ 0 & 1 & y_d \\ 0 & 0 & 1 \end{bmatrix} \quad (11)$$

$$K = \begin{bmatrix} k_1 & 0 & 0 \\ 0 & k_2 & 0 \\ 0 & 0 & 1 \end{bmatrix} \quad (12)$$

$$R = \begin{bmatrix} \cos \theta & -\sin \theta & 0 \\ \sin \theta & \cos \theta & 0 \\ 0 & 0 & 1 \end{bmatrix} \quad (13)$$

where k_1, k_2 are scale factors in x -coordinate and y -coordinate, respectively, θ is the deflection angle, x_d, y_d are translation displacements. Then each point of C^* , $[x, y, 1]^T$ needs to be traced back to $[x, y]^T$, and so we update C^* .

3.3.2. Choosing the characteristic points from P and C* for match

The characteristic points-set Z is chosen from the ones that are particular in position. Here we choose the special boundary points and points on cupped surface to construct the set Z .

$$Z = \left\{ (\vec{a}_i, \vec{b}_i) \mid \vec{a}_i \in C^*, \vec{b}_i \in P, \vec{a}_i \text{ and } \vec{b}_i \text{ have the same feature} \right\}. \quad (14)$$

3.3.3. Matching images composed of P and C*.

1) Matching the characteristic points-set Z , the result is obtained by: $\min \sum_{i=1}^k (\vec{a}_i - \vec{b}_i)^2$

2) Matching images with the criteria:

- The image of C^* should not be beyond Pb ;
- The area covered by the image of C^* should be as large as possible.

3) Modify the value of neighbours number k , to achieve the optimal match.

3.3.4. Embedding C* into the points-set P to form the points-set H and obtain the new 2D image

Here *embedding* is referred to lying points of C^* and P into the same coordinate, as is shown in Figure 3.

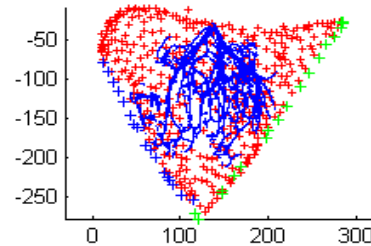


Figure 3. the image of H , which is embedded C^* into P

3.4. Inverse Mapping from 3D curve surface to 2D plane of LV

Based on the idea of the LLE algorithm, points of H is inversely mapped to the 3D structure by means of the locally linear relationship among points:

1) Points of C^* are put as the data X_i , whose neighbour points-set is P . That means, to find the neighbour points of each 2D PFN point.

2) W_{ij} of the inverse mapping is computed, before each point of C^* will be linearly described by P . For each point of P can be expressed by points in 3D ventricular points-set F , then C^* can be linearly expressed by points of F .

Thereby, the 2D anatomical PFN data information is embedded into the 3D ventricular structure. Thus we finished the construction of 3D PFN structure. The result is shown as in Figure. 4.

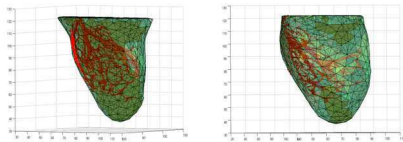


Figure 4. the construction of the PFN in the LV from different sides

4. Discussion and conclusions

The construction of an anatomically based network of canine Purkinje fibers, which takes advantages of using real anatomical data of the ventricular entity, has been described. It aims at keeping the locally linear relationship between points in the entity by means of applying manifold learning to constructing the inner linear-shaped structure of a closed curve surface, and then reconstructing PFN based on the anatomical entity.

The Purkinje fiber network, one of the most important part of the ventricular conduction system, is reproduced based on the real data, instead of using manually drawing or approximate shape. The mapping between the curve surface and the plane is successfully performed, which

makes the 3D structure of PFN could be efficiently and completely reconstructed from the 2D PFN image.

Acknowledgements

The work is partially supported by the National High-tech Research and Development Program of China ("863" Program) under Grant No. 2006AA01Z308 and the National Natural Science Foundation of China (NSFC) under Grant Nos. 60571025 and 60872099.

References

- [1] Siregar P, Sinteff JP, Julen N, Beux PL. An interactive 3d anisotropic cellular automata model of the heart. *Comput. Biomed* 1998; 31: 323–347.
- [2] Simelius K, Nenonen J, Horacek M. Modeling cardiac ventricular activation. *Int. J. Bioelectromagn* 2001; 3: 51–58.
- [3] Vigmond EJ, Clements CJ. Construction of a computer model to investigate sawtooth effects in the Purkinje system. *IEEE TBME* 2007; 54: 389–399.
- [4] Tenenbaum JB, Silva V, Langford JC. A global geometric framework for nonlinear dimensionality reduction. *Science* 2000; 290: 2319 – 2323.
- [5] S.T.Roweis, L.K. Saul. Nonlinear dimensionality reduction by local linear embedding. *Science* 2000; 290: 2323–2326.
- [6] Saul LK, Roweis ST. Think globally, fit locally: unsupervised learning of low dimensional manifolds. *Journal of Machine Learning Research* 2003; 4: 119-155.
- [7] David LD, Carrie G. Hessian eigenmaps: new locally linear embedding techniques for high dimensional data, TR2003-08, Dept. of Statistics, Stanford University, 2003.

Address for correspondence

Kuanquan Wang
Mailbox 332,
School of Computer Science and Technology
Harbin Institute of Technology,
No. 92, West Da Zhi street, Harbin, China
150001
wangkq@hit.edu.cn